Biomaterials xxx (2010) 1–11

Contents lists available at ScienceDirect

Biomaterials

journal homepage: www.elsevier.com/locate/biomaterials

Directed 3D cell alignment and elongation in microengineered hydrogels

Hug Aubin [a,b,1], Jason W. Nichol [a,b,1], Ché B. Hutson [a,b], Hojae Bae [a,b], Alisha L. Sieminski [c], Donald M. Cropek [d], Payam Akhyari [e], Ali Khademhosseini [a,b,*]

[a] Center for Biomedical Engineering, Department of Medicine, Brigham and Women's Hospital, Harvard Medical School, 65 Landsdowne Street, Cambridge, MA 02139, USA
[b] Harvard-MIT Division of Health Sciences and Technology, Massachusetts Institute of Technology, Cambridge, MA 02139, USA
[c] Franklin W. Olin College of Engineering, Needham, MA 02492, USA
[d] U.S. Army Corps of Engineers, Construction Engineering Research Laboratory, Champaign, IL 61822, USA
[e] University Hospital of Duesseldorf, Department of Cardiovascular Surgery, Duesseldorf, Germany

ARTICLE INFO

Article history:
Received 28 April 2010
Accepted 21 May 2010
Available online xxx

Keywords:
Tissue engineering
Micropatterning
Cellular alignment
3D engineered tissue

ABSTRACT

Organized cellular alignment is critical to controlling tissue microarchitecture and biological function. Although a multitude of techniques have been described to control cellular alignment in 2D, recapitulating the cellular alignment of highly organized native tissues in 3D engineered tissues remains a challenge. While cellular alignment in engineered tissues can be induced through the use of external physical stimuli, there are few simple techniques for microscale control of cell behavior that are largely cell-driven. In this study we present a simple and direct method to control the alignment and elongation of fibroblasts, myoblasts, endothelial cells and cardiac stem cells encapsulated in microengineered 3D gelatin methacrylate (GelMA) hydrogels, demonstrating that cells with the intrinsic potential to form aligned tissues *in vivo* will self-organize into functional tissues *in vitro* if confined in the appropriate 3D microarchitecture. The presented system may be used as an *in vitro* model for investigating cell and tissue morphogenesis in 3D, as well as for creating tissue constructs with microscale control of 3D cellular alignment and elongation, that could have great potential for the engineering of functional tissues with aligned cells and anisotropic function.

1. Introduction

Controlled cellular alignment plays a crucial role in the microarchitecture of many human tissues, dictating their biological and mechanical function. For example in native myocardial tissue, the complex organization of cardiomyocytes and fibroblasts within the cardiac extracellular matrix (ECM) is critical to the electrical and mechanical properties of the heart [1]. Musculoskeletal tissue is similarly organized, with myoblasts forming highly aligned muscle fibers through fusion into multi-nucleated myotubes [2]. This specific arrangement of differentiated myocytes within the musculoskeletal ECM is essential for the generation of contractile force. In a broad range of additional tissues of the human body, from the vasculature [3] to connective tissue [4], tissue function is also dictated by cellular organization. Thus, to effectively study and replicate the biological function of many native tissues *in vivo*, engineered tissues must recapitulate these native 3D microstructures *in vitro*.

Engineered tissue constructs are typically generated by embedding cells in synthetic or biological 3D scaffolds [5]. However, in previous studies, the inability to precisely control cell behavior has often resulted in poor cell and ECM organization within engineered constructs. Such tissue constructs had limited ability to recreate complex tissues characterized by precise cell and ECM alignment. Microscale technologies have been successfully integrated into many tissue engineering applications and have allowed for enhanced control of cell behavior and function through control of the cellular microenvironment [6]. Many critical components of the cellular microarchitecture, such as cell elongation [7,8], cell differentiation [9,10], cell–cell contacts and signaling [11,12], can all be modulated through control of the microenvironment. The combination of microengineering with hydrogels having tunable cell responsivity, mechanical stiffness, and microarchitecture, has enabled a whole new range of complementary applications and model systems for controlling and investigating cell behavior [13].

Significant research has been directed towards controlling the spatial organization of cells in defined microarchitectures. A multitude of techniques have been described to control 2D cellular

* Corresponding author. Center for Biomedical Engineering, Department of Medicine, Brigham and Women's Hospital, Harvard Medical School, 65 Landsdowne Street, Cambridge, MA 02139, USA.
E-mail address: alik@rics.bwh.harvard.edu (A. Khademhosseini).
[1] These authors contributed equally to this work.

0142-9612/$ – see front matter © 2010 Elsevier Ltd. All rights reserved.
doi:10.1016/j.biomaterials.2010.05.056

alignment on micro- and nanostructured surfaces produced either by chemical or topographic patterning [14–18]. Nonetheless, surface patterns or channels are limited to inducing cellular alignment in 2D. Controlling the organization of cells within a 3D cell population in engineered constructs still remains a major challenge. In some cases cellular alignment within cell-laden 3D scaffolds has been induced through mechanical [19–21] or electrical stimulation [22–24], however there are few simple options to recreate complex 3D cellular architectures *in vitro* without the need for external cell stimuli. One such system of cell-laden collagen hydrogels in micromolded polydimethylsiloxane (PDMS) channels demonstrated controlled cell alignment in 3D, however the hydrogels remained confined in the PDMS channels, therefore limiting its possible applications [25]. There is a need for simple, 3D systems for controlling cellular alignment on the microscale without the need for external stimulation or guidance systems for a wide range of applications from tissue engineering to investigating and controlling cellular behaviors such as differentiation and function.

In this work, we present a simple and direct method to control cellular organization in 3D using cells encapsulated in cell-responsive, microengineered hydrogels. This system could be used as an *in vitro* model for investigating cell and tissue morphogenesis, or could form the basis for the creation of complexly organized engineered tissues. We hypothesized that solely through precise control of the microgeometry, achieved by micropatterning cell-laden 3D gelatin methacrylate (GelMA) hydrogels into high aspect ratio rectangular constructs, that we could induce controlled cellular alignment and elongation throughout the entire engineered construct. The described system is applicable to many different cell types and can be used to engineer tissue constructs of user-defined size and shape with microscale control of cellular organization, which could form the basis for constructing 3D engineered tissues with specific elongation and alignment *in vitro*.

2. Materials and method

2.1. Materials

The chemicals for gelatin methacrylate (GelMA) (Gelatin (Type A, 300 bloom from porcine skin) and methacrylic anhydride), pretreatment of glass slides ((3-trimethoxysilyl) propyl methacrylate (TMSPMA) and polyethylene glycol diacrylate (PEG)) were all purchased from Sigma–Aldrich (Wisconsin, USA). Glass slides and coverslips were purchased from Fisher Scientific (Pennsylvania, USA). Photolithography printed photomasks were purchased from CADart (Washington, USA), while the UV light source (Omnicure S2000) was purchased from EXFO Photonic Solutions Inc. (Ontario, Canada). Digital calipers from Marathon Watch Company Ltd (Ontario, Canada) were used to determine the thickness of the spacers.

2.2. Gelatin methacrylate synthesis

GelMA was synthesized as previously described [26–28]. A "high" degree of methacrylation was achieved by using 20% (v/v) of methacrylic anhydride in the GelMA synthesis reaction as previously demonstrated [28]. Samples were then dialyzed in 12–14 kDa cutoff dialysis tubing in distilled water for 1 week at 40 °C, and subsequently lyophilized for 1 week.

2.3. Cell culture

All cells were cultured in a standard cell culture incubator (Forma Scientific) in a 5% CO_2 atmosphere at 37 °C. NIH 3T3-fibroblasts were maintained in Dulbecco's modified Eagle medium (DMEM; Gibco) supplemented with 10% fetal bovine serum (FBS), 1% Penicillin/Streptomycin (P/S) and were passaged twice per week. Immortalized, GFP-expressing human umbilical vein endothelial cells (HUVEC) were maintained in endothelial basal medium (EBM-2; Lonza) supplemented with endothelial growth BulletKit (Lonza), 1% P/S and were passaged when 60-70% confluence was reached while media was exchanged every 2 days. Immortalized rodent myoblasts (C2C12) were maintained in DMEM supplemented with 20% FBS, 1% P/S, 1% L-Glutamine and were passaged when 60–70% confluence was reached. Cardiac side population cells (CSP) were received at passage 5 after isolation (generous gift from the Ronglih Liao group), maintained in α-modified Eagle medium (α-MEM) supplemented with 20% FBS, 1% P/S, passaged when 60–70% confluence was reached and were used at passage 7 for cell encapsulation studies. Immortalized human liver carcinoma cells (Hep-G2) were maintained in DMEM supplemented with 10% FBS, 1% P/S and were passaged twice per week.

2.4. Prepolymer preparation

GelMA macromers were combined with DPBS (Gibco) and 0.5% (w/v) photoinitiator (2-hydroxy-1-(4-(hydroxyethoxy) phenyl)-2-methyl-1-propanone, Irgacure 2959, CIBA Chemicals), incubated at 80 °C until fully dissolved and subsequently used for cell encapsulation studies. PEG (MW: 1000) prepolymer (20% (w/v) in DPBS) was used to coat TMSPMA treated glass slides as previously described [28].

2.5. Cell encapsulation and micropatterning

Cell-laden GelMA hydrogels were micropatterned onto PEG coated glass slides using techniques previously demonstrated [28]. Briefly, 10 μL of 20% (w/v) PEG prepolymer was pipetted between a TMSPMA coated glass slide and an untreated coverslip (18 mm (w) × 18 mm (l)), then exposed to 6.9 mW/cm^2 UV light (360–480 nm) for 50 s. Following polymerization, the coverslip was removed and PEG coated slides were used for cell-laden GelMA micropattern formation to prevent cell adhesion to the slide surface.

For encapsulation studies, cells were trypsinized, counted and resuspended in 5% (w/v) GelMA prepolymer at a density of 10 million cells per mL. One droplet (40 μL) of the prepolymer cell suspension was pipetted between a PEG coated glass slide and an untreated coverslip separated by 150 μm high spacers. The photomask was placed directly on top of the coverslip prior to exposure to 6.9 mW/cm^2 UV light (360–480 nm) for 20 s. Subsequently the coverslip was removed and the remaining unpolymerized prepolymer cell suspension was gently washed away with preheated DPBS. Micropatterned, cell-laden hydrogels were cultured for up to one week in 6-well-plates (Fisher Scientific) under standard culture conditions, using the specified media for each cell type, with the media exchanged every 48 h. To visualize micropattern fidelity Rhodamine B (Fluka, 479.02 Da) was mixed with GelMA prepolymer without cells at a concentration of 0.2 mM prior to UV exposure in order to produce fluorescently-labeled hydrogels.

2.6. Quantification of cellular alignment and elongation

After 5 days in culture, cell-laden hydrogels were formalin-fixed and stained with phalloidin (Alexa-Fluor 594, Invitrogen) and DAPI according to the manufacturers instructions to visualize filamentous F-actin and cell nuclei, respectively. Whole constructs were visualized with an inverted microscope (Nikon TE 2000-U, Nikon instruments inc., USA) for phase contrast images and a confocal microscope (Leica SP5, Leica Microsystems, Wetzlar, Germany) for fluorescence images. The nuclear shape index and alignment of DAPI stained nuclei were measured to quantitatively evaluate overall cell elongation and alignment as previously demonstrated [29,30]. The nuclear alignment angles, defined as the orientation of the major elliptic axis of individual nuclei with respect to the horizontal axis, were measured using built-in functions of NIH ImageJ software. All nuclear alignment angles were then normalized to the respective preferred nuclear orientation defined as the mean orientation of all nuclei per sample. For analysis, alignment angles were subsequently grouped in 10° increments with respect to the preferred nuclear orientation, with all cells within less then 10° considered to be aligned as previously described [31]. Additionally, the shape index (circularity $= 4^*\pi^*$area/perimeter^2) of each individual cell nucleus determining nuclear elongation was evaluated using built-in functions of NIH ImageJ software, with a shape index of 1 representing a circle.

2.7. MMP inhibition and MMP activity quantification

To suppress the enzymatic activity of the matrix metalloproteinases (MMPs) secreted by 3T3-fibroblasts, culture media was supplemented with the general MMP inhibitor doxycycline at a concentration of 400 μM. Doxycycline at similar concentrations has previously been shown to inhibit MMP expression and activation without significantly affecting cell function or viability [32,33]. The quantity of MMP-2 and MMP-9 protein in media was determined using gelatin zymography as previously described [33,34]. Following 4 days culture, specimens (25 μL) from culture media of the cell-laden microconstructs, were electrophoresed on 10% SDS gels containing 1% gelatin, renaturated in 2.5% Triton X-100 (v/v), incubated overnight at 37 °C and stained with Coomassie blue R-250 to visualize enzymatic activity (all reagents and gels from Bio-Rad). The corresponding bands were visualized, quantified, normalized by MMP-2/MMP-9 standards (Chemicon/Millipore, Billerica, MA) and assessed using built-in functions of NIH ImageJ software.

2.8. Statistical analysis

Statistical significance was determined for replicates of 5 by an independent Student *t*-test for two groups of data or analysis of variance (ANOVA) followed by Bonferroni's post-hoc test for multiple comparisons using SPSS statistical software package Version 16.0 (SPSS Inc. Chicago, USA). Data are represented as mean ± standard deviation (SD).

Please cite this article in press as: Aubin H, et al., Directed 3D cell alignment and elongation in microengineered hydrogels, Biomaterials (2010), doi:10.1016/j.biomaterials.2010.05.056

3. Results

3.1. Cellular alignment and elongation in micropatterned cell-laden 3D hydrogels

Previous studies have reported that fibroblasts encapsulated in macroscale, partially constrained collagen gels self-organized along local tension lines [35] and more importantly, elongated along free boundaries [36]. From those and previous 2D studies from our group describing the behavior of cell alignment on grooved surfaces [16,17] and microfibers [18] we hypothesized that by controlling the microgeometry of cell-responsive, cell-laden 3D hydrogels we could induce controlled cellular organization leading to aligned, 3D microconstructs achieved solely through micropatterned geometric restriction without the need to apply additional stimuli.

In the present study, we encapsulated 3T3-fibroblasts at a cell density of 10×10^6 cells/mL in 150 μm tall GelMA microconstructs of varying widths using a photolithographic technique. Multiple parallel microconstructs of a defined width surrounded by a 1 mm border to serve as an unpatterned control were created using a 1 cm × 1 cm mask (Fig. 1A). A GelMA macromer concentration of 5% (w/v) with a methacrylation degree of roughly 80% was chosen because of its robust mechanical stiffness and decreased mass swelling ratio despite short UV exposure making it suitable for micropatterning intricate cell-laden shapes, while maintaining cell viability [28]. In addition, comparable GelMA macromer concentrations have demonstrated rapid and extensive cellular proliferation, remodeling and reorganization in 3D [28], while viability has been shown to decrease with macromer concentration in other, similar hydrogel systems [37,38].

Similiarly to previous studies, the micropatterned hydrogels showed high pattern fidelity and high initial cell viability of encapsulated fibroblasts in both patterned and unpatterned cell-laden hydrogels (data not shown) [27,28]. After 24 h of culture the 3T3-fibroblasts started to actively elongate and proliferate inside the GelMA hydrogels, completely filling the hydrogels with cells by day 5 of culture (Fig. 1B). While the cellular orientation remained random in the unpatterned hydrogels, fibroblasts significantly self-organized into highly aligned microconstructs consisting of elongated, aligned cells in the micropatterned hydrogels. Cellular orientation followed the major axis of the rectangular microconstructs demonstrating that this behavior could be directed. Though at early time points, alignment was largely limited to the fibroblasts closest to the edge surfaces of the micropatterns, this effect quickly spread throughout the entire construct within 4–5 days. In addition to these qualitative observation, quantitative analysis of nuclear alignment at different heights of the microconstructs, showing roughly 60% of aligned cells (Fig. 2), supported the assertion that similar and significant cell elongation and alignment was occurring throughout the entire thickness of the patterned microconstructs, making it a controlled 3D phenomenon. Using lower initial cell densities for encapsulation or higher GelMA macromer concentrations to generate micropatterned cell-laden 3D hydrogels showed similar cellular orientation and cellular elongation phenomena, however the time needed to create hydrogels that were completely filled with elongated and aligned cells was increased (data not shown). Therefore, the data suggest that the elongation and alignment responses could be controlled and directed through optimization of the cell and hydrogel concentrations and culture time.

3.2. Effect of microgeometry

Quantitative analysis of cellular alignment and elongation in cell-laden hydrogels following 5 days of culture revealed a strong influence of the microgeometry on 3D cellular organization. We varied the width of the patterned rectangular microconstructs from 50 μm to 200 μm, while maintaining the same height and length for all microconstructs as shown above. The nuclear alignment and shape index were measured using NIH ImageJ software to quantitatively evaluate overall cell alignment and elongation as previously demonstrated [29,30]. All cells whose nuclei were within 10° of the preferred nuclear orientation were considered to be aligned as previously described [31].

Statistical analysis demonstrated that controlling the width of the constructs using micropatterning significantly increased cell alignment (Fig. 3). In 50 μm wide microconstructs, 64 ± 8% of the cells were aligned (Fig. 3A), with roughly 90% of the cells aligned within 20° of the preferred nuclear orientation (Fig. 3F). Increasing the width of the micropatterns to 100 μm or 200 μm decreased the alignment to 40 ± 6%, and 31 ± 8% of the cells, respectively (Fig. 3A). While cellular alignment in the 50 μm wide microconstructs was significantly greater than all other conditions ($p < 0.001$), the 100 μm wide microconstructs also showed a significant difference

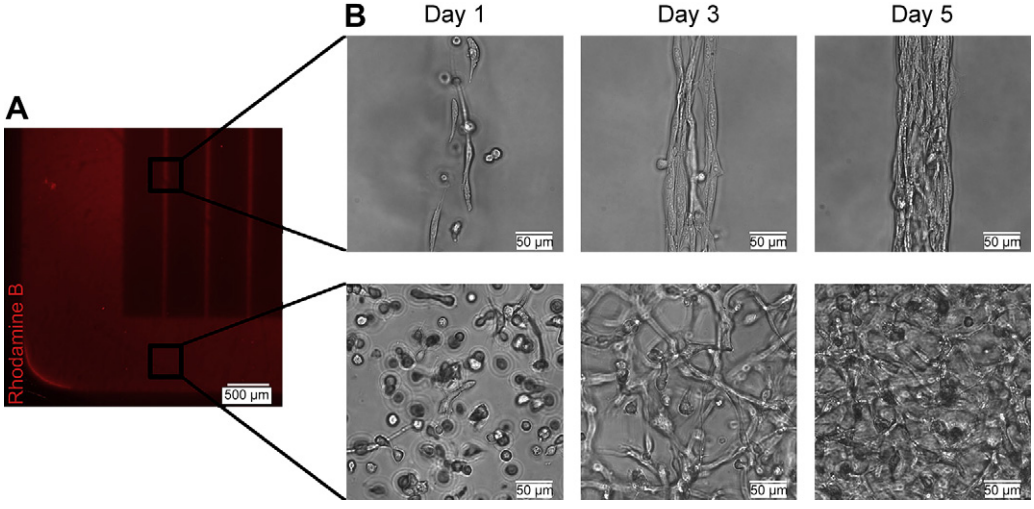

Fig. 1. Cell morphology and organization as a function of time in patterned and unpatterned microconstructs. Patterning 3T3-fibroblast-laden 5% GelMA hydrogels into high aspect ratio rectangular microconstructs (50 μm (w) × 800 μm (l) × 150 μm (h)) induced cellular alignment and elongation, while cellular orientation in unpatterned hydrogels remained random. (A) Rhodamine B stained GelMA hydrogel construct shows the patterned and unpatterned regions. (B) Representative phase contrast images of 3T3-fibroblasts (10×10^6 cells/mL) encapsulated in patterned (top row) and unpatterned regions of the GelMA hydrogel (bottom row) on days 1, 3 and 5 of culture show that elongation increases over time for all hydrogels, while alignment is only induced in patterned constructs.

Please cite this article in press as: Aubin H, et al., Directed 3D cell alignment and elongation in microengineered hydrogels, Biomaterials (2010), doi:10.1016/j.biomaterials.2010.05.056

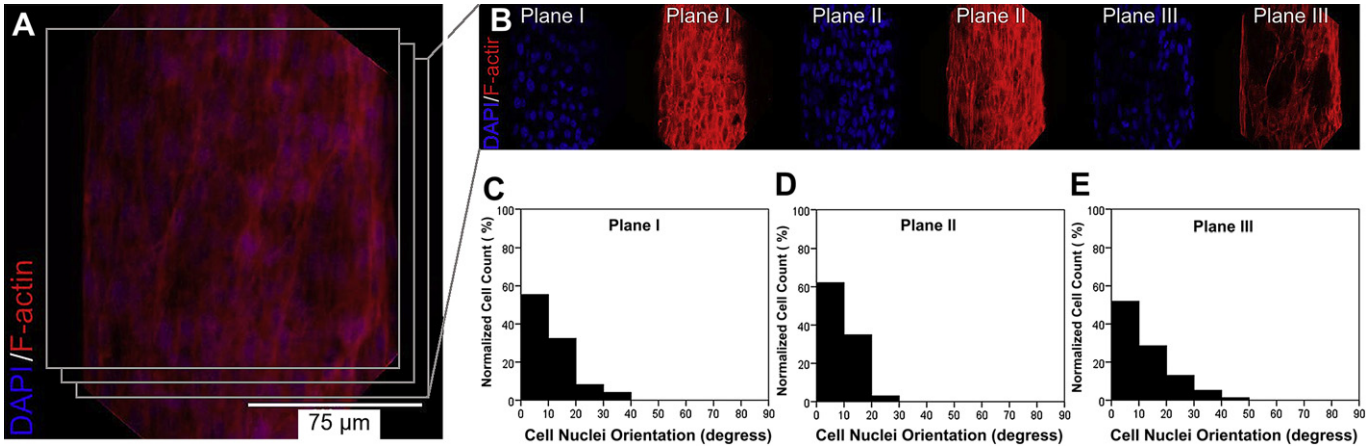

Fig. 2. Multilayer analysis of cell alignment. Cellular alignment in 3T3-fibroblast-laden 5% GelMA hydrogels patterned into high aspect ratio rectangular microconstructs (50 μm (w) × 800 μm (l) × 150 μm (h)) was maintained throughout the entire height of the construct. (A) Representative DAPI/F-actin stained 3D-projection (50 μm z-stack) of a 3T3-laden rectangular microconstruct after 5 days of culture. (B) Three DAPI and F-actin stained xy-planes from the microconstruct (distance: 10 μm in z-plane) with corresponding histograms ((C), (D) and (E) respectively) showing the nuclear alignment in 10° increments relative to the preferred nuclear orientation of each individual plane demonstrates similar alignment along the major axis throughout the thickness of the constructs.

from the unpatterned hydrogels ($p < 0.01$). In contrast the 200 μm wide microconstructs did not show significant alignment. Cells in unpatterned hydrogels displayed random orientation with only 19 ± 9% of the cells being within 10° of the mean nuclear orientation of the construct (Fig. 3A). One-way ANOVA analysis confirmed that there was a main effect of the micropattern width in driving cell alignment ($p < 0.001$). With increasing feature size only cells in close proximity to the perimeter or surface appeared to align along the long-axis of the micropatterns, while random organization dominated away from the edge surfaces as the microconstruct width increased (Fig. 3G–J). Histograms of cellular alignment angles displaying the relative percentages of cells within 10° increments further demonstrated that relative alignment decreased with increasing width (Fig. 3C–F).

Generally, cell alignment inside the hydrogel correlated well with nuclear elongation. The nuclei of cells inside the 50 μm wide rectangular microconstructs were the most elongated, with the lowest mean nuclear shape index of 0.807 ± 0.02, as compared to all other groups ($p < 0.01$) (Fig. 3B). The 100 μm wide micropatterns displayed a mean nuclear shape index of 0.869 ± 0.03, while the 200 μm wide micropatterns displayed a mean nuclear shape index of 0.917 ± 0.02 and the unpatterned hydrogels a mean nuclear shape index of 0.923 ± 0.03 (Fig. 3B). Similar to the cellular alignment behavior, the 100 μm wide microconstructs showed a significant decrease in the nuclear shape index as compared to unpatterned hydrogels ($p < 0.05$) while the 200 μm wide micropatterns failed to show a significant difference compared to the unpatterned controls (Fig. 3B). Also similar to the behavior seen in the cell alignment analysis, one-way ANOVA revealed a main effect of the micropatterns' width in driving cell elongation ($p < 0.001$).

3.3. Effect of MMP activity

Matrix metalloproteinases (MMPs) are ECM-specific enzymes used by fibroblasts, and many other cells, to adapt to changes in their microenvironment through ECM remodeling. During the remodeling processes cell elongation and locomotion occurs, partially due to generation of traction forces through actin cell cytoskeleton reorganization [39]. Since this cell-generated tension is hypothesized to drive the spatial orientation and morphology of cells embedded in gels [35], we inhibited MMP activity with 400 μM doxycycline, as previously described [32,33], to determine the effect of ECM remodeling *via* MMP activity on 3D cellular alignment and elongation of 3T3-fibroblasts encapsulated in 50 μm wide GelMA microconstructs. To verify the inhibition, MMP-2 and MMP-9 activity in the media of microconstructs both with and without supplementation was determined after 48 h culture *via* gelatin zymography (Fig. 4A). Normalizing the band intensity of each sample to that of the unsupplemented media, MMP-2 activity decreased by 38 ± 10% and MMP-9 activity decreased by 22 ± 6% in the doxycycline supplemented media ($p < 0.001$) (Fig. 4B).

MMP inhibition considerably decreased cellular alignment inside the patterned rectangular microconstructs ($p < 0.001$). Only 29 ± 7% of the cells were aligned within 10° of the preferred orientation, showing no significant difference as compared to the unpatterned hydrogels that were either doxycycline treated (19 ± 7%) or untreated (19 ± 9%) (Fig. 4C). Upon closer analysis there still appeared to be a trend toward increased cellular alignment despite MMP inhibition with 54% ± 15% of the nuclei oriented within 20°, but not 10°, of the preferred orientation in micropatterned constructs as compared to only 31% ± 7% of alignment within 20° of the unpatterned hydrogels ($p < 0.05$) (Fig. 4E–F). Analysis of variance by two-way ANOVA revealed a main effect of micropatterning, as well as MMP inhibition and an interaction between both, in driving the alignment ($p < 0.001$). Similarly, MMP inhibition raised the mean nuclear shape index to 0.933 ± 0.01 ($p < 0.001$) in the micropatterned hydrogels and to 0.960 ± 0.01 in the unpatterned hydrogels decreasing cellular elongation even as compared to the unpatterned hydrogels without MMP inhibition (Fig. 4D).

Interestingly, there was a significant difference in cell elongation ($p < 0.05$) between the patterned and unpatterned hydrogels supplemented with doxycycline. This suggested that microscale control of micropattern width still enhanced cellular elongation, although to a lesser degree, even in the presence of MMP inhibition. This was confirmed by analysis of variance by two-way ANOVA revealing a main effect of the micropatterning, in addition to the MMP inhibition and an interaction between the two conditions, in driving the elongation ($p < 0.001$). These findings suggest that ECM remodeling *via* MMP activity plays an important role in cellular alignment and elongation of the micropatterned fibroblast-laden 3D hydrogels.

3.4. Effect of cell type

To assess if this simple 3D alignment method is applicable for engineering a variety of tissues, we evaluated the capacity to induce cellular alignment and enhance cellular elongation in different cell

Please cite this article in press as: Aubin H, et al., Directed 3D cell alignment and elongation in microengineered hydrogels, Biomaterials (2010), doi:10.1016/j.biomaterials.2010.05.056

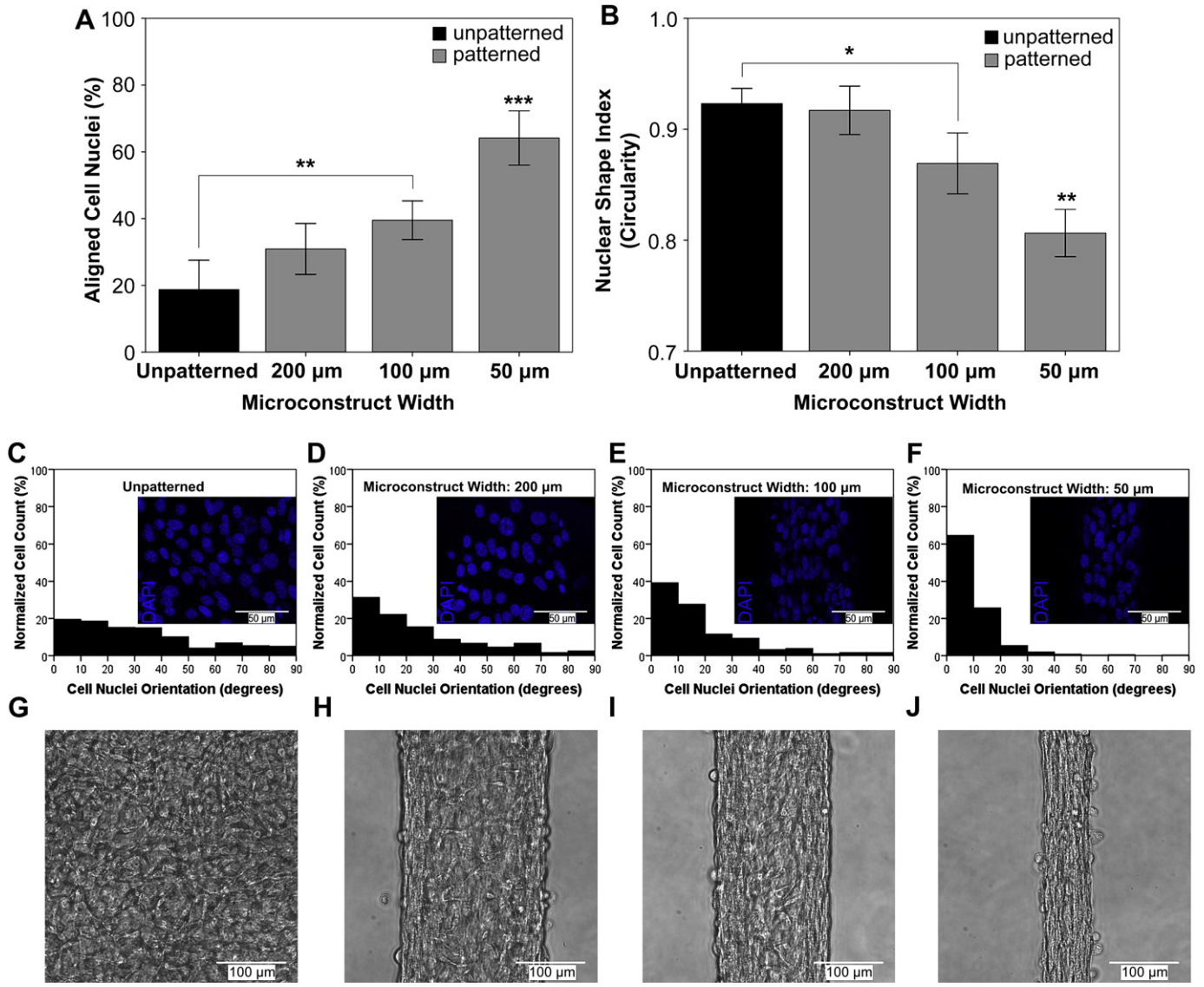

Fig. 3. Cell elongation and alignment as a function of microconstruct width. Decreasing the width of patterned rectangular 5% GelMA microstructures (800 μm (l) × 150 μm (h)) increased 3T3-fibroblast alignment as well as nuclear elongation after 5 days of culture. (A) Mean percentage of aligned cell nuclei (within 10° of preferred nuclear orientation) shows 100 μm constructs were significantly more aligned than unpatterned controls, while 50 μm constructs were significantly more aligned than all other groups. (B) Mean nuclear shape index (circularity = $4*\pi*$area/perimeter^2) shows a similar pattern with 100 μm constructs having a significantly lower index than unpatterned controls, while 50 μm constructs were significantly different than all other groups. (C), (D), (E) and (F) Histograms of the relative alignment in 10° increments demonstrates increased cellular alignment with decreased microconstruct width. (G), (H), (I) and (J) Representative phase contrast images of unpatterned, 200 μm, 100 μm and 50 μm wide microconstructs respectively show significantly increased cell alignment and elongation inside the constructs with decreasing width. (Error bars: ± SD; $^{***}p < 0.001$; $^{**}p < 0.01$; $^{*}p < 0.01$).

types. Human umbilical vein endothelial cells (HUVEC) were chosen as a model cell type for the potential applications in vascularized tissue engineering, rodent myoblasts (C2C12) were investigated for potential skeletal muscle tissue engineering applications and rodent cardiac side population cells (CSP) were evaluated for myocardial tissue engineering applications. All of these potential applications demand highly elongated, organized and aligned ECM-cell constructs to mimic the complexly organized microarchitecture *in vivo*. Additionally we investigated the cellular behavior of encapsulated human liver carcinoma cells (Hep-G2) in micropatterned hydrogels as a control, as Hep-G2 cells, in contrast to the cell types above, do not align or elongate *in vivo* or *in vitro*. All cell types were encapsulated in 5% (w/v) GelMA hydrogels and micropatterned into 50 μm wide rectangular microconstructs under the same conditions as used for the 3T3-fibroblast encapsulation studies. Cell viability was similar to the encapsulated 3T3-fibroblasts (data not shown).

Quantitative analysis showed a significant difference in both cellular alignment and elongation with micropatterned encapsulation for HUVEC, C2C12 and CSP cells as compared to unpatterned cell-laden hydrogels. Staining the cell-laden gels for F-actin (Fig. 5A–B) revealed highly aligned, elongated and interconnected cell structures for the HUVEC, C2C12 and CSP cells along the major axis of the micropatterned hydrogels. Actin fiber intensity and organization appeared to be substantially reduced in the unpatterned hydrogels, being confined only to the nuclei located near the edges of the hydrogels, especially for the C2C12 and CSP cells. Analysis of variance by two-way ANOVA revealed that both micropatterning and cell type had a significant effect on cell alignment and elongation, as well as displaying an interactive effect ($p < 0.001$). Cellular orientation in the unpatterned hydrogels remained random, independent of cell type, with approximately 20% of the cells being aligned within the preferred orientation. In contrast, micropatterned constructs showed 51 ± 11% alignment

Please cite this article in press as: Aubin H, et al., Directed 3D cell alignment and elongation in microengineered hydrogels, Biomaterials (2010), doi:10.1016/j.biomaterials.2010.05.056

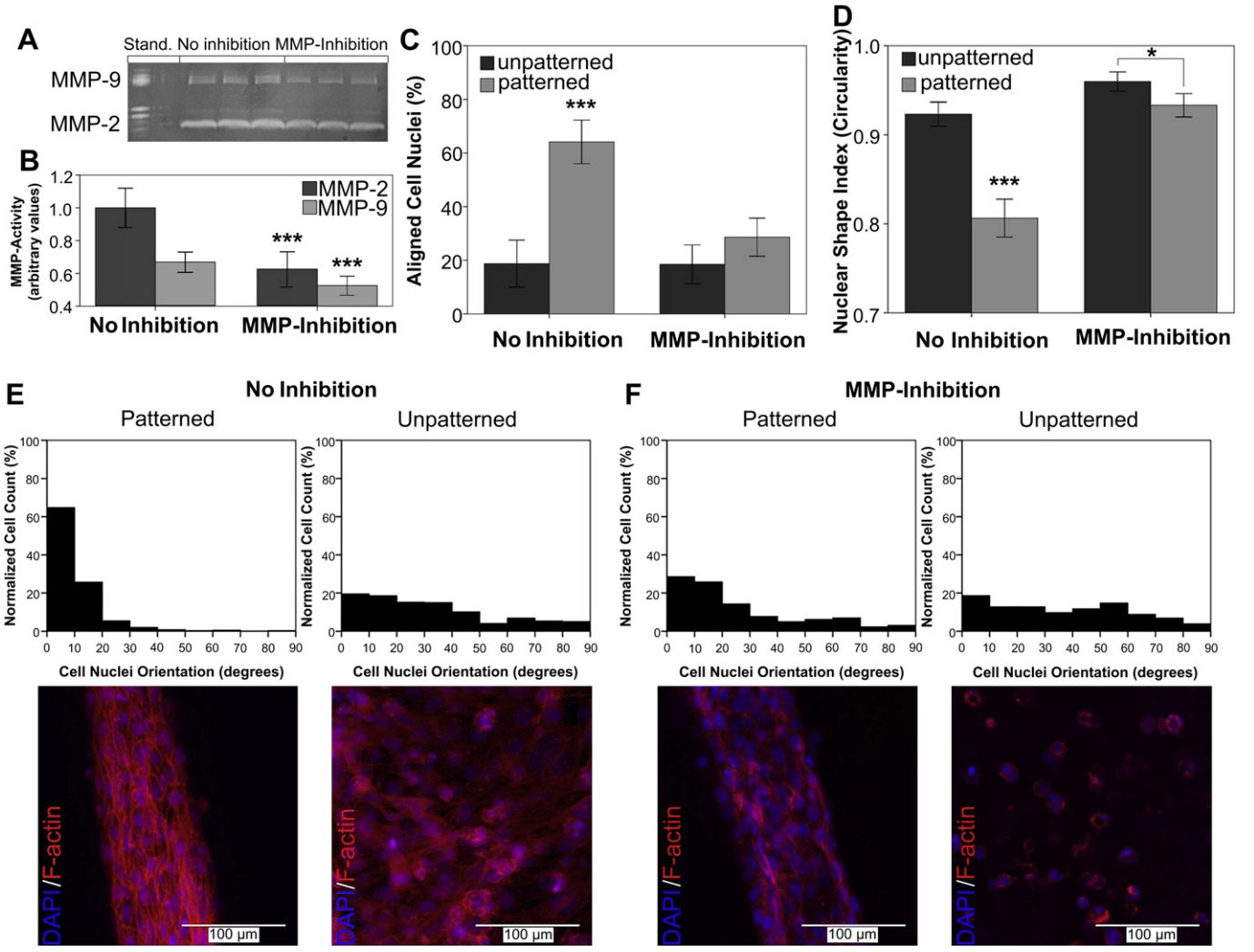

Fig. 4. Effect of MMP inhibition on elongation and alignment in patterned microconstructs. General MMP inhibition with doxycycline supplemented media (400 μM) for 4 days of culture decreased nuclear alignment and elongation in 3T3-fibroblast-laden 5% GelMA hydrogels patterned into high aspect ratio rectangular microconstructs (50 μm (w) × 800 μm (l) × 150 μm (h)) and showed no differences to unpatterned hydrogels with and without MMP inhibition. (A) Zymogram showing MMP-2 and MMP-9 activity in culture media of cell-laden micropatterned hydrogels compared to human standard. (B) Normalized MMP-2 and MMP-9 activity of unsupplemented and supplemented samples demonstrates significant decreases in MMP expression and activity with inhibition. (C) Mean cell nuclei alignment (within 10° of preferred nuclear orientation) shows decreased alignment with MMP inhibition. (D) Mean nuclear shape index (circularity = $4^{*}\pi^{*}$area/perimeter^2) similarly shows decreased cell elongation with MMP inhibition, however micropatterned constructs show significantly greater elongation than unpatterned controls. (E) and (F) Histograms showing the percentage of aligned cell nuclei in 10° increments, with representative z-stack overlays of DAPI/F-actin staining of microconstructs cultured in unsupplemented and supplemented media respectively. (Error bars: ± SD; $^{***}p < 0.001$; $^{*}p < 0.01$).

with HUVEC cells ($p < 0.001$), 41 ± 10% alignment with C2C12 cells ($p < 0.001$) and 45 ± 10% alignment with CSP cells ($p < 0.001$) (Fig. 5C). Extending the range of preferred nuclear orientation to within 20° substantially increased the percentage of aligned cells to 77% for HUVEC cells, 60% for C2C12 cells and 63% for CSP cells (histograms not shown). The mean nuclear shape index was determined to be greater than 0.920 for all three cell types in unpatterned hydrogels, while patterned microconstructs displayed a mean nuclear shape index of 0.877 ± 0.02 for HUVEC cells ($p < 0.01$), 0.834 ± 0.04 for C2C12 cells ($p < 0.01$) and 0.820 ± 0.04 for CSP cells ($p < 0.01$), demonstrating a significant increase in cellular elongation in the micropatterned hydrogels (Fig. 5D).

As expected Hep-G2 cells failed to self-organize into aligned constructs even if patterned into high aspect ratio microconstructs (Fig. 5A–B). There was no significant difference between the patterned and unpatterned hydrogels with respect to cellular alignment (19 ± 7% vs. 19 ± 4% respectively) or cellular elongation (0.941 ± 0.01 vs. 0.938 ± 0.01 respectively) (Fig. 5C–D). DAPI and F-actin staining showed Hep-G2 cells forming cell clusters of multiple cell nuclei independent of the microgeometry. These data confirmed our initial hypothesis that an intrinsic potential to organize into aligned tissues *in vivo* is a necessary prerequisite to induce cellular alignment and enhance cellular elongation when stimulated by specific microgeometrical features.

3.5. Self-assembled and aligned 3D tissue constructs

Interestingly, it was observed that cell-laden microconstructs appeared to increase in width with increasing culture time. We quantitatively evaluated this phenomenon for 3T3-fibroblasts encapsulated in 50 μm wide microconstructs (Fig. 6). To account for swelling, the rectangular microconstructs were allowed to reach equilibrium over the first 24 h of culture [28], after which the mean construct width of multiple replicates was recorded every 24 h and measured using NIH ImageJ software. After 4 days of culture the mean construct width increased roughly by 40 μm from day 1 ($p < 0.001$) (Fig. 6A). Qualitative analysis of the resulting images suggested that this phenomenon was due to cell proliferation, as

Please cite this article in press as: Aubin H, et al., Directed 3D cell alignment and elongation in microengineered hydrogels, Biomaterials (2010), doi:10.1016/j.biomaterials.2010.05.056

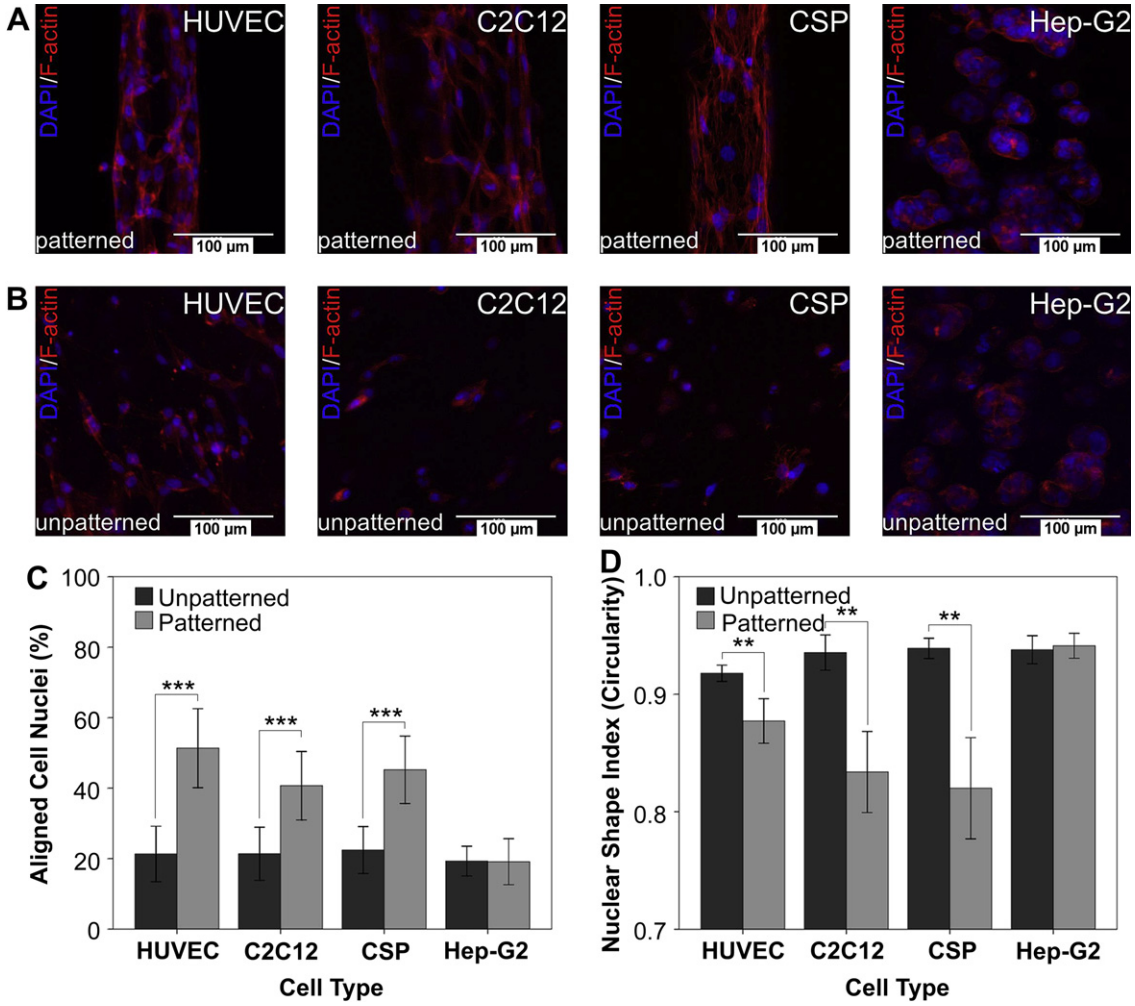

Fig. 5. Control of cell elongation and alignment in multiple cell types. Patterning cell-laden 5% GelMA hydrogels into rectangular microconstructs (50 μm (w) × 800 μm (l) × 150 μm (h)) induced cellular alignment and elongation after 5 days of culture only in cell types possessing an intrinsic potential to organize into aligned tissues *in vivo*, while cellular orientation in unpatterned parts of the same hydrogels remained random. Representative z-stack overlays of DAPI/F-actin staining of (A) patterned and (B) unpatterned hydrogels laden with HUVEC, C2C12, CSP, and Hep-G2 cells respectively show patterning induced aligned and elongated cell-network formations in HUVEC, C2C12 and CSP cells and patterning independent cell-cluster formations in Hep-G2 cells. (C) Mean percentage of aligned cell nuclei (within 10° of preferred nuclear orientation) shows that patterned HUVEC-, C2C12- and CSP-laden constructs were significantly more aligned than unpatterned controls, while in Hep-G2-laden constructs patterning failed to induce cell alignment. (D) Mean nuclear shape index (circularity = $4^*\pi^*$area/perimeter^2) similarly shows that patterned HUVEC-, C2C12- and CSP-laden constructs were significantly more elongated than unpatterned controls, while in Hep-G2-laden constructs patterning failed to induce cell elongation. (Error bars: ± SD; $^{**}p < 0.01$; $^{***}p < 0.001$).

over time the 3T3-fibroblast laden microconstructs showed increased cellularity on the microconstruct edges while maintaining the cellularity and cell morphology inside the construct.

Based on this observation, we hypothesized that by reducing the spacing between cell-laden microconstructs, that this expansion could lead to microconstructs contacting and merging together, yielding a macroscale aligned tissue. We further hypothesized that, given sufficient time, close enough proximity and through control of micro- and macroscale geometry, the result would be self-assembled and aligned 3D tissue constructs of user-defined shape and size. When multiple 50 μm wide 3T3-fibroblast-laden microconstructs were cultured 200 μm apart, regions of microconstructs began merging together by day 4 of culture, forming points of contact between neighboring constructs (Fig. 7A, red arrows). By day 7 of culture all the micropatterns had converged together into a macroscale tissue construct of roughly 1 cm^2 (Fig. 7B). While the initial rectangular micropatterns could still be distinguished as aligned micropillars within the tissue construct, the space that originally existed between the microconstructs was now fully filled with an organized cellular network. F-actin staining of the whole tissue construct showed actin fiber orientation in single direction, aligned along the long-axis of the original micropatterns throughout the entire construct (Fig. 7C). Fiber alignment was not only restricted to the micropillars but was also displayed by the majority of the newly formed cellular networks between the micropillars throughout the entire thickness of the tissue construct. Therefore, we demonstrated, by simply varying the spacing of parallel microconstructs, we were able to create customized, macroscale, cell-laden 3D hydrogels with controlled cellular alignment and elongation in all three dimensions.

4. Discussion

Engineered tissues designed to mimic native tissues must recreate the complex 3D cellular distribution and organization found *in vivo*, while maintaining the cell viability and function of the emulated tissues. While we, and others, have demonstrated the ability to control cell behavior on patterned 2D surfaces [14–18], controlling cellular organization in 3D tissue models still remains a challenge. Here we present a novel, robust method to control cellular alignment and elongation of cells encapsulated in cell-responsive, 3D hydrogels solely by specific control of the hydrogel

Please cite this article in press as: Aubin H, et al., Directed 3D cell alignment and elongation in microengineered hydrogels, Biomaterials (2010), doi:10.1016/j.biomaterials.2010.05.056

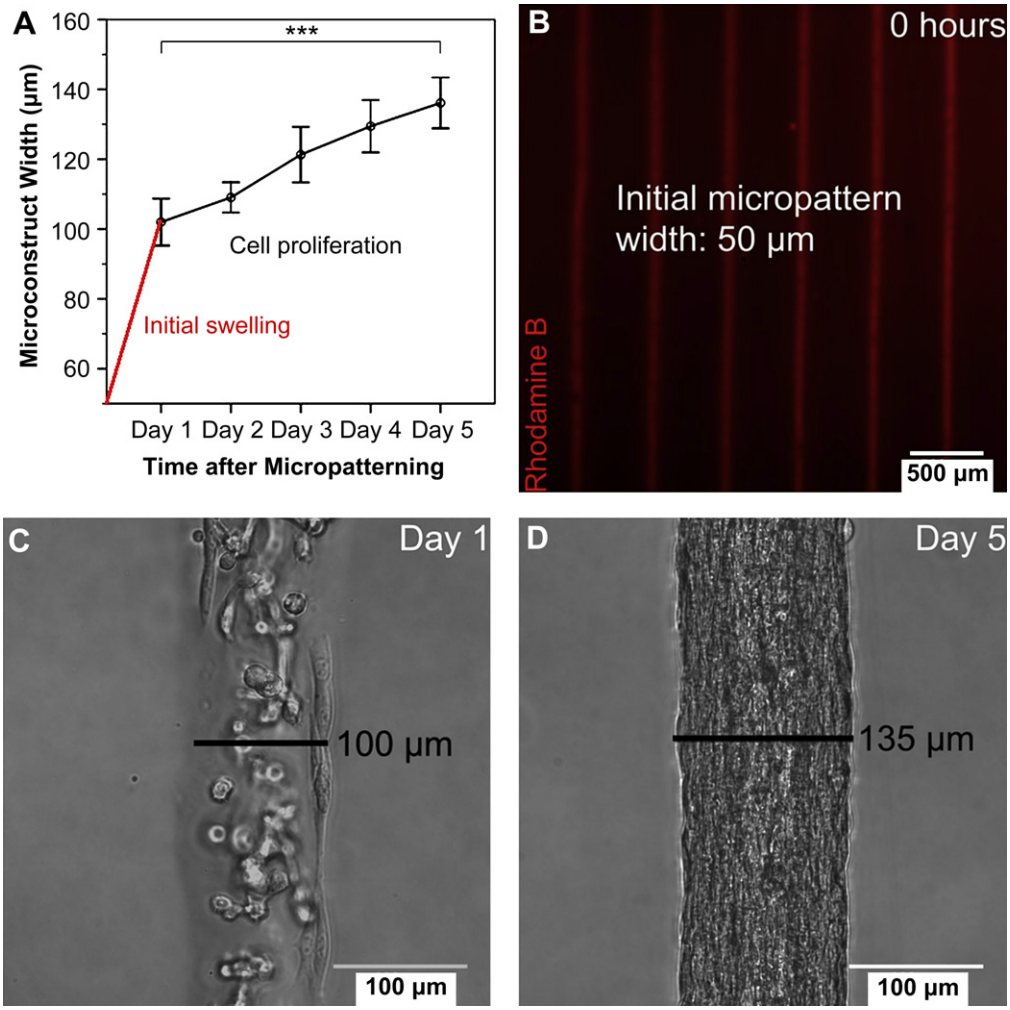

Fig. 6. Microconstruct width as a function of time in patterned cell-laden hydrogels. 3T3-fibroblast-laden 5% GelMA hydrogels patterned into rectangular microconstructs (50 μm (w) × 800 μm (l) × 150 μm (h)) increased in width after initial swelling due to cell proliferation. (A) Mean microconstruct width at each culture day after initial 24 h swelling period shows increase in feature size. (B) Rhodamine B stained hydrogel construct demonstrates the initial micropattern width of 50 μm directly after patterning. (C) and (D) Representative phase contrast images of a single microconstruct at day 1 and 5 respectively show increase in feature size due to cell proliferation. (Error bars: ± SD; $^{***}p < 0.001$).

geometry and without the need for any external stimuli or guidance. This work represents a significant step forward in our ability to create functional tissues *in vitro*, enabling simple and direct microscale control of 3D cellular organization, while also providing a powerful model system for investigating cell and tissue morphogenesis *in vitro*.

External stimuli, e.g. mechanical stretch [19–21], electrical impulse [22–24] and flow-induced shear stress [40,41], have been previously demonstrated to induce cellular alignment in 3D cell-laden scaffold materials. However, this often requires elaborate, macroscale stimulation systems, which could potentially have limited control of cellular organization on the microscale. Other attempts to control cellular organization in 3D microenvironments without external stimuli have been reported previously by using laser photolithography to pattern biomolecules in 3D hydrogels creating predefined pathways for cell migration [42,43]. The focus and intensity of the laser are the limiting factors in the spatial resolution of biomolecule distribution making this method unsuitable for the creation of complex functional tissues. A recent method using a highly focused two-photon laser (TPL) beam to micropattern cell adhesive ligands (RGDS) in 3D scaffolds allows for greater control over spatial RGDS distribution [44]. The TPL photolithographic technique, however, has a very low RGDS to hydrogel conjugation efficiency and the optimal RGDS concentrations for directed cell locomotion still need to be determined.

Although bioactive hydrogels have shown the ability to guide cell migration, it has yet to be demonstrated that this method can be used to create complex and organized functional tissues. Norman and Desai introduced a method to control cellular alignment in cell-laden 3D hydrogels using a physically predefined pathway [25]. Using microfabrication techniques a fibroblast-seeded collagen matrix was molded around parallel polydimethylsiloxane (PDMS) channels that served as an internal skeleton to guide the cells to grow in a prescribed 3D pattern. In their study, the fibroblasts elongated and organized along the direction of the channels throughout the height of the scaffold. However, the applicability for tissue engineering applications of the described system could be limited due to the presence and persistence of the internal PDMS skeleton, as well as the limited feature thickness commonly associated with PDMS micromolding.

In this work, we demonstrated that cells encapsulated in cell-responsive, microengineered hydrogels could self-organize without additional support or guidance into highly aligned 3D cellular networks solely through confinement in the appropriate microgeometrical conditions. This technique does not require external physical stimuli or predefined pathways inside the

Please cite this article in press as: Aubin H, et al., Directed 3D cell alignment and elongation in microengineered hydrogels, Biomaterials (2010), doi:10.1016/j.biomaterials.2010.05.056

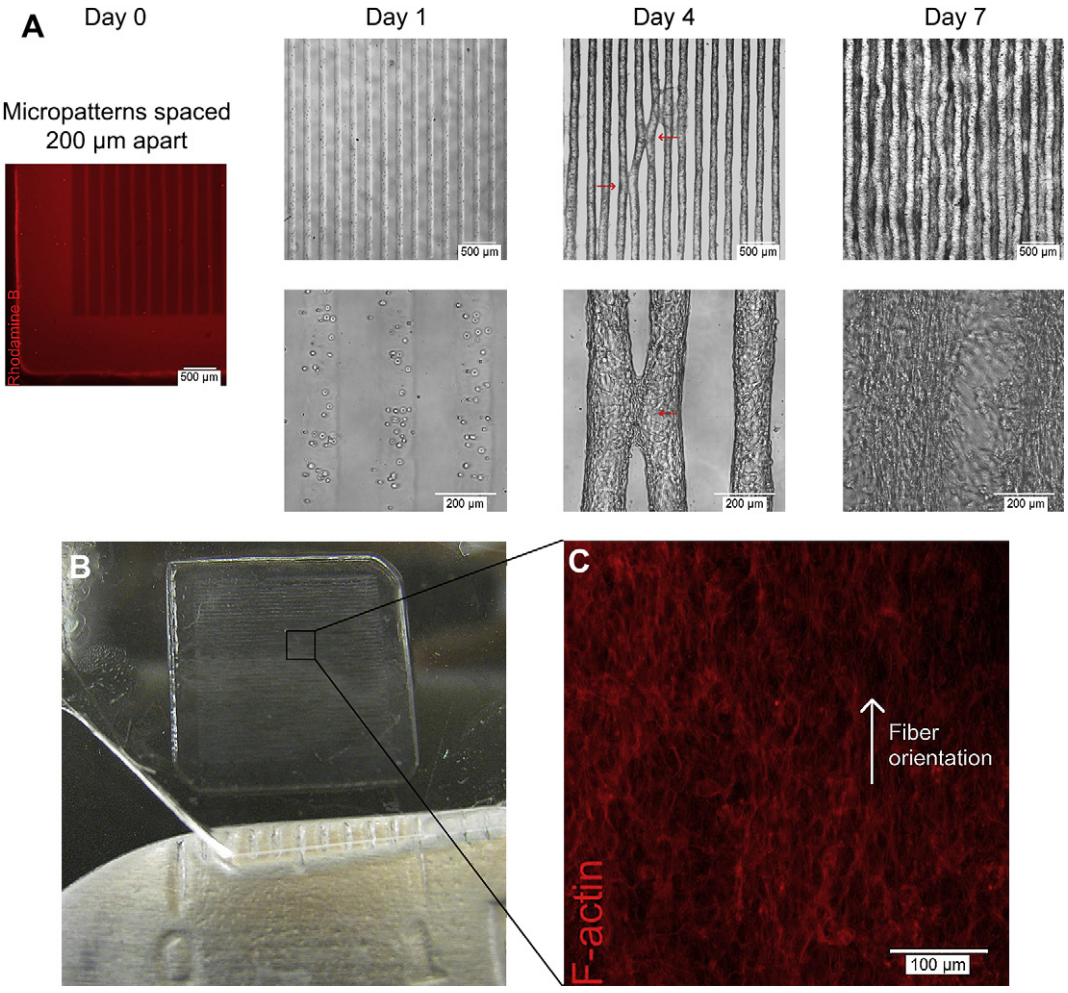

Fig. 7. Self-assembly of multiple aligned microconstructs into a macroscale and aligned 3D tissue construct. 3T3-fibroblast-laden 5% GelMA hydrogels patterned into rectangular microconstructs (50 μm (w) × 800 μm (l) × 150 μm (h)) spaced 200 μm apart self-assembled into macroscale and aligned 3D tissue constructs after 7 days of culture through convergence of multiple, aligned microconstructs. (A) Rhodamine B stained hydrogel shows initial microconstruct spacing of 200 μm at day 0; representative phase contrast images of cell-laden microconstructs at day 1, 4 and 7 respectively show focal points of contact between neighboring aligned microconstructs at day 4 (red arrows) and convergence into a macroscale 3D tissue construct at day 7. (B) Image of a 1 cm × 1 cm, self-assembled 3D tissue construct at day 7. (C) Representative F-Actin staining of middle xy-plane of macroscale 3D tissue construct shows orientated actin fiber organization in single direction.

hydrogel. Therefore, this approach presents the first simple and direct method to create highly aligned, engineered microtissues through the elegant exploitation of the cells' intrinsic potential to self-organize into functional 3D tissues in a suitable micro-architectural environment. The intrinsic cellular potential to organize into aligned tissues *in vivo* was demonstrated to be a necessary prerequisite to alignment in this system, as evidenced by the behavior of Hep-G2 cells encapsulated in micropatterned hydrogels. These data suggest that confined 3D microarchitectures do not induce cellular alignment and elongation *per se*, but only do so in cell types which exist in elongated and aligned arrangements *in vivo*. Raghavan et al. recently showed that endothelial tubulogenesis could be controlled through spatially patterning endothelial cells within micromolded collagen gels using similar feature sizes as the micropatterns presented in this study [45], further suggesting that increased cellular alignment and elongation of cells embedded in defined microarchitectures also enhances organization into complex, functional networks.

The presented data demonstrated that one of the key mechanisms required for cells to align in this system was ECM remodeling *via* MMP-2 and MMP-9 expression. This further confirms our previous findings that increased MMP-2 expression, and especially activation, improved cardiomyocyte alignment and elongation in unpatterned engineered myocardial constructs [33]. It has additionally been shown previously that inhibiting the MMP activity of fibroblasts encapsulated in collagen gels correlates with a significant reduction in collagen gel contraction without affecting the maximum tension generated by the cells respective to MMP activity [46]. This, combined with our data showing that MMP inhibition significantly reduces cellular alignment of encapsulated fibroblasts, further suggests that cell-generated traction forces work in conjunction with MMP-mediated ECM remodeling in controlling the cellular alignment. More in depth investigation using this system could potentially increase our knowledge about complex cell interaction and organization within 3D cell populations in well-defined microarchitectures.

In this study, cellular alignment correlated strongly with a significant increase in cell elongation. The described results analyzed nuclear elongation and alignment as a method to demonstrate overall cellular morphology. Nuclear elongation has been demonstrated to correlate with cell differentiation [30] as the cell shape formed by cytoskeletal assembly also facilitates nuclear shape distortion. Elongated nuclei have been shown to promote DNA synthesis and influence nucleocytoplasmatic transport rates, hence improving cellular function [47,48]. Lee et al. recently demonstrated that human embryonic stem cells can be driven to

Please cite this article in press as: Aubin H, et al., Directed 3D cell alignment and elongation in microengineered hydrogels, Biomaterials (2010), doi:10.1016/j.biomaterials.2010.05.056

differentiate selectively into a neuronal lineage on nanoscale ridge/groove patterns without the use of any differentiation inducing agents [49]. As additional studies have showed a similar effect of control of 2D alignment of stem cells promoting specific cellular differentiation in stem cell systems [50–54], we hypothesize that the cell-laden hydrogels with well-defined microgeometries presented in this study might be used to control differentiation within a 3D stem cell population and to further investigate the underlying differentiation mechanisms.

The presented system demonstrated the potential to engineer macroscale 3D tissue constructs of user-defined size and shape with microscale control of cellular elongation and alignment through convergence of multiple, aligned microconstructs. Varying the 3D geometry and assembling multiple, aligned 3D building blocks of equal, different or combined cell types in a "bottom up" approach offers further possibilities to mimic the microarchitecture of complexly organized functional tissues [55]. When combined with the demonstrated applicability to many different cell types, the described techniques could have great potential for *in vitro* engineering of tissues requiring a high degree of cellular alignment and anisotropic function such as cardiac, nervous, musculoskeletal and vascular tissues.

5. Conclusions

In this study we presented a simple and direct method for microscale control of cellular alignment and elongation for cells encapsulated in cell-responsive, 3D hydrogels solely through specific control of the hydrogel geometry. This was achieved by exploiting the cells' innate tendency both to align along free surfaces and to align with neighboring cells. In addition, this was done without the need for any additional external physical stimuli or internal guidance systems. Our data suggests that cells possessing an intrinsic potential to organize into aligned tissues *in vivo* also can be directed to self-organize into aligned tissue constructs *in vitro* if confined in suitable 3D microarchitectures *via* ECM remodeling through MMP activity. This simple method is applicable to many different cell types giving the ability to create customized, macroscale, 3D tissue constructs with microscale control of cellular alignment and elongation. This represents a significant step forward in our ability to create engineered functional tissues *in vitro* with specific microarchitectural features, while also providing a powerful model for investigating cell and tissue morphogenesis.

Acknowledgments

This paper was supported by the National Institutes of Health (DE019024; HL092836), the National Science Foundation CAREER Award (DMR0847287) and the Office of Naval Research Young Investigator Award. H. A. was supported by the Biomedical Exchange Program from the International Academy of Life Sciences (BMEP/IALS). J.W.N. was supported by the U.S. Army Construction Engineering Research Laboratory, Engineering Research and Development Center (USACERL/ERDC).

Appendix

Figures with essential color discrimination. All of the figures in this article have parts that are difficult to interpret in black and white. The full colour images can be found in the on-line version, at doi:10.1016/j.biomaterials.2010.05.056.

References

[1] Papadaki M, Bursac N, Langer R, Merok J, Vunjak-Novakovic G, Freed LE. Tissue engineering of functional cardiac muscle: molecular, structural, and electrophysiological studies. Am J Physiol Heart Circ Physiol 2001;280(1):H168–78.
[2] Wigmore PM, Dunglison GF. The generation of fiber diversity during myogenesis. Int J Dev Biol 1998;42(2):117–25.
[3] Chiu JJ, Chen LJ, Chen CN, Lee PL, Lee CI. A model for studying the effect of shear stress on interactions between vascular endothelial cells and smooth muscle cells. J Biomech 2004;37(4):531–9.
[4] Vunjak-Novakovic G, Altman G, Horan R, Kaplan DL. Tissue engineering of ligaments. Annu Rev Biomed Eng; 2004:6131–56.
[5] Khademhosseini A, Vacanti JP, Langer R. Progress in tissue engineering. Sci Am 2009;300(5):64–71.
[6] Khademhosseini A, Langer R, Borenstein J, Vacanti JP. Microscale technologies for tissue engineering and biology. Proc Natl Acad Sci U S A 2006;103(8):2480–7.
[7] Chen CS, Mrksich M, Huang S, Whitesides GM, Ingber DE. Geometric control of cell life and death. Science 1997;276(5317):1425–8.
[8] McBeath R, Pirone DM, Nelson CM, Bhadriraju K, Chen CS. Cell shape, cytoskeletal tension, and RhoA regulate stem cell lineage commitment. Dev Cell 2004;6(4):483–95.
[9] Burdick JA, Vunjak-Novakovic G. Engineered microenvironments for controlled stem cell differentiation. Tissue Eng Part A 2009;15(2):205–19.
[10] Murtuza B, Nichol JW, Khademhosseini A. Micro- and nanoscale control of the cardiac stem cell niche for tissue fabrication. Tissue Eng Part B Rev 2009;15(4):443–54.
[11] Nelson CM, Chen CS. Cell–cell signaling by direct contact increases cell proliferation via a PI3K-dependent signal. FEBS Lett 2002;514(2–3):238–42.
[12] Nelson CM, Liu WF, Chen CS. Manipulation of cell–cell adhesion using bowtie-shaped microwells. Methods Mol Biol; 2007:3701–10.
[13] Khademhosseini A, Langer R. Microengineered hydrogels for tissue engineering. Biomaterials 2007;28(34):5087–92.
[14] Hasirci V, Kenar H. Novel surface patterning approaches for tissue engineering and their effect on cell behavior. Nanomedicine (Lond) 2006;1(1):73–90.
[15] Lim JY, Donahue HJ. Cell sensing and response to micro- and nanostructured surfaces produced by chemical and topographic patterning. Tissue Eng 2007;13(8):1879–91.
[16] Khademhosseini A, Eng G, Yeh J, Kucharczyk PA, Langer R, Vunjak-Novakovic G, et al. Microfluidic patterning for fabrication of contractile cardiac organoids. Biomed Microdevices 2007;9(2):149–57.
[17] Manbachi A, Shrivastava S, Cioffi M, Chung BG, Moretti M, Demirci U, et al. Microcirculation within grooved substrates regulates cell positioning and cell docking inside microfluidic channels. Lab Chip 2008;8(5):747–54.
[18] Hwang CM, Park Y, Park JY, Lee K, Sun K, Khademhosseini A, et al. Controlled cellular orientation on PLGA microfibers with defined diameters. Biomed Microdevices 2009;11(4):739–46.
[19] Akhyari P, Fedak PW, Weisel RD, Lee TY, Verma S, Mickle DA, et al. Mechanical stretch regimen enhances the formation of bioengineered autologous cardiac muscle grafts. Circulation 2002;106(12 Suppl. 1):I137–42.
[20] Vader D, Kabla A, Weitz D, Mahadevan L. Strain-induced alignment in collagen gels. Plos One 2009;4(6):e5902.
[21] Nguyen TD, Liang R, Woo SL, Burton SD, Wu C, Almarza A, et al. Effects of cell seeding and cyclic stretch on the fiber remodeling in an extracellular matrix-derived bioscaffold. Tissue Eng Part A 2009;15(4):957–63.
[22] Radisic M, Park H, Shing H, Consi T, Schoen FJ, Langer R, et al. Functional assembly of engineered myocardium by electrical stimulation of cardiac myocytes cultured on scaffolds. Proc Natl Acad Sci U S A 2004;101(52):18129–34.
[23] Flaibani M, Boldrin L, Cimetta E, Piccoli M, De Coppi P, Elvassore N. Muscle differentiation and myotubes alignment is influenced by micropatterned surfaces and exogenous electrical stimulation. Tissue Eng Part A 2009;15(9):2447–57.
[24] Tandon N, Cannizzaro C, Chao PH, Maidhof R, Marsano A, Au HT, et al. Electrical stimulation systems for cardiac tissue engineering. Nat Protoc 2009;4(2):155–73.
[25] Norman JJ, Desai TA. Control of cellular organization in three dimensions using a microfabricated polydimethylsiloxane-collagen composite tissue scaffold. Tissue Eng 2005;11(3–4):378–86.
[26] Van Den Bulcke AI, Bogdanov B, De Rooze N, Schacht EH, Cornelissen M, Berghmans H. Structural and rheological properties of methacrylamide modified gelatin hydrogels. Biomacromolecules 2000;1(1):31–8.
[27] Benton JA, Deforest CA, Vivekanandan V, Anseth KS. Photocrosslinking of gelatin macromers to synthesize porous hydrogels that promote valvular interstitial cell function. Tissue Eng Part A 2009;15(11):3221–30.
[28] Nichol JW, Koshy S, Bae H, Hwang CM, Yamanlar S, Khademhosseini A. Cell-laden microengineered gelatin methacrylate hydrogels. Biomaterials 2010;31(21):5536–44.
[29] Charest JL, García AJ, King WP. Myoblast alignment and differentiation on cell culture substrates with microscale topography and model chemistries. Biomaterials 2007;28(13):2202–10.
[30] Brammer KS, Oh S, Cobb CJ, Bjursten LM, van der Heyde H, Jin S. Improved bone-forming functionality on diameter-controlled TiO(2) nanotube surface. Acta Biomater 2009;5(8):3215–23.

[31] Charest JL, Eliason MT, García AJ, King WP. Combined microscale mechanical topography and chemical patterns on polymer cell culture substrates. Biomaterials 2006;27(11):2487–94.
[32] Franco C, Ho B, Mulholland D, Hou G, Islam M, Donaldson K, et al. Doxycycline alters vascular smooth muscle cell adhesion, migration, and reorganization of fibrillar collagen matrices. Am J Pathol 2006;168(5):1697–709.
[33] Nichol JW, Engelmayr GC, Cheng M, Freed LE. Co-Culture induces alignment in engineered cardiac constructs via MMP-2 expression. Biochem Biophys Res Commun 2008;373(3):360–5.
[34] Galis ZS, Johnson C, Godin D, Magid R, Shipley JM, Senior RM, et al. Targeted disruption of the matrix metalloproteinase-9 gene impairs smooth muscle cell migration and geometrical arterial remodeling. Circ Res 2002;91(9):852–9.
[35] Klebe RJ, Caldwell H, Milam S. Cells transmit spatial information by orienting collagen fibers. Matrix 1989;9(6):451–8.
[36] Costa KD, Lee EJ, Holmes JW. Creating alignment and anisotropy in engineered heart tissue: role of boundary conditions in a model three-dimensional culture system. Tissue Eng 2003;9(4):567–77.
[37] Du Y, Lo E, Ali S, Khademhosseini A. Directed assembly of cell-laden microgels for fabrication of 3D tissue constructs. Proc Natl Acad Sci U S A 2008;105(28):9522–7.
[38] Yeh J, Ling Y, Karp JM, Gantz J, Chandawarkar A, Eng G, et al. Micromolding of shape-controlled, harvestable cell-laden hydrogels. Biomaterials 2006;27(31):5391–8.
[39] Pollard TD, Cooper JA. Actin, a central player in cell shape and movement. Science 2009;326(5957):1208–12.
[40] Ng CP, Swartz MA. Fibroblast alignment under interstitial fluid flow using a novel 3-D tissue culture model. Am J Physiol Heart Circ Physiol 2003;284(5):H1771–7.
[41] Pedersen JA, Lichter S, Swartz MA. Cells in 3D matrices under interstitial flow: effects of extracellular matrix alignment on cell shear stress and drag forces. J Biomech 2010;43(5):900–5.
[42] Hern DL, Hubbell JA. Incorporation of adhesion peptides into nonadhesive hydrogels useful for tissue resurfacing. J Biomed Mater Res 1998;39(2):266–76.
[43] Luo Y, Shoichet MS. A photolabile hydrogel for guided three-dimensional cell growth and migration. Nat Mater 2004;3(4):249–53.
[44] Lee SH, Moon JJ, West JL. Three-dimensional micropatterning of bioactive hydrogels via two-photon laser scanning photolithography for guided 3D cell migration. Biomaterials 2008;29(20):2962–8.
[45] Raghavan S, Nelson CM, Baranski JD, Lim E, Chen CS. Geometrically controlled endothelial tubulogenesis in micropatterned gels. Tissue Eng Part A, in press.
[46] Phillips JA, Vacanti CA, Bonassar LJ. Fibroblasts regulate contractile force independent of MMP activity in 3D-collagen. Biochem Biophys Res Commun 2003;312(3):725–32.
[47] Maniotis AJ, Chen CS, Ingber DE. Demonstration of mechanical connections between integrins, cytoskeletal filaments, and nucleoplasm that stabilize nuclear structure. Proc Natl Acad Sci U S A 1997;94(3):849–54.
[48] Getzenberg RH, Pienta KJ, Ward WS, Coffey DS. Nuclear structure and the three-dimensional organization of DNA. J Cell Biochem 1991;47(4):289–99.
[49] Lee MR, Kwon KW, Jung H, Kim HN, Suh KY, Kim K, et al. Direct differentiation of human embryonic stem cells into selective neurons on nanoscale ridge/groove pattern arrays. Biomaterials 2010;31(15):4360–6.
[50] Shimizu K, Fujita H, Nagamori E. Alignment of skeletal muscle myoblasts and myotubes using linear micropatterned surfaces ground with abrasives. Biotechnol Bioeng 2009;103(3):631–8.
[51] Engel E, Martínez E, Mills CA, Funes M, Planell JA, Samitier J. Mesenchymal stem cell differentiation on microstructured poly (methyl methacrylate) substrates. Ann Anat 2009;191(1):136–44.
[52] Sridharan I, Kim T, Wang R. Adapting collagen/CNT matrix in directing hESC differentiation. Biochem Biophys Res Commun 2009;381(4):508–12.
[53] Zhao F, Veldhuis JJ, Duan Y, Yang Y, Christoforou N, Ma T, et al. Low oxygen tension and synthetic nanogratings improve the uniformity and stemness of human mesenchymal stem cell layer. Mol Ther 2010;18(5):1010–8.
[54] Yin Z, Chen X, Chen JL, Shen WL, Hieu Nguyen TM, Gao L, et al. The regulation of tendon stem cell differentiation by the alignment of nanofibers. Biomaterials 2010;31(8):2163–75.
[55] Nichol JW, Khademhosseini A. Modular tissue engineering: engineering biological tissues from the bottom up. Soft Matter 2009;5(7):1312–9.

Please cite this article in press as: Aubin H, et al., Directed 3D cell alignment and elongation in microengineered hydrogels, Biomaterials (2010), doi:10.1016/j.biomaterials.2010.05.056